Teleoperation Mappings from Rigid Link Robots to Their Extensible Continuum Counterparts

Chase G. Frazelle[†], Apoorva D. Kapadia, Katelyn E. Fry, and Ian. D. Walker

Abstract— We present a novel approach to teleoperation of continuum robots. In contrast to previous approaches restricted to three Degree-of-Freedom (DoF) joysticks, a six degree-of-freedom rigid-link manipulator is used as the input device. Mappings from the rigid-link arm to the continuum robot are synthesized and analyzed, focusing on their potential for creating a more intuitive operational interface. The approach was implemented using a six degree-of-freedom rigid-link manipulator as input device for teleoperation of a three section, nine degree-of-freedom continuum robot. Tests were conducted across a range of planar and spatial tasks, using fifteen participant operators. The results demonstrate the feasibility of the approach, and suggest that it can be effective independent of the prior robotics, gaming, or teleoperative experience of the operator.

I. Introduction

Teleoperation has traditionally been, and remains, a key enabling element in implementation of many robotic systems, and is particularly important in many safety-critical operations and unstructured environments [1]. Teleoperation of robot manipulators has been the subject of extensive research through the years [1]. However, almost all the related literature on teleoperation of manipulators applies to conventional rigid-link robot structures. In this paper, we instead consider the teleoperation of continuum robots.

Continuous backbone, or continuum robots [2], differ fundamentally from traditional rigid-link robot structures, due to their ability to change shape (bend) at any point along their structure. Inspired by invertebrate morphologies in nature (tongues, trunks, and tentacles), their structures give them the ability to penetrate environments and perform tasks convention robots cannot [3], [4]. Over the past twenty years or so, an ever increasing number and variety of continuum robots have been designed and implemented [5]. They have found applications in numerous medical procedures [6], [7], [8], inspection operations [9], space [10], [11], and underwater environments [12], [13].

The state of the art in modeling and operation of continuum robots has advanced rapidly in the past few years. The kinematics of continuum robots has been extensively studied [14], [15]. Research specific to continuum robots in areas traditional to robotics such as dynamics [16], [17], [18], [19], [20], [21], contact modeling [22], [23], motion planning [24], [25], [26], [27], and control [28], [29], [30], [31],

[32], [33] is currently very active. However, little attention has been paid to the issue of user interfaces for, and in particular teleoperation of, continuum robots [5]. Human operation of continuum robots is hampered by the fact that their movements are typically significantly less intuitive to operators than those of their rigid-link counterparts.

To the best of the authors knowledge, only one work focusing on teleoperation modalities for continuum robots [34] has been reported in the literature. In that paper, a series of teleoperation mappings from conventional gaming joysticks (two or three degrees-of-freedom devices) to motions of a continuum robot were evaluated. While the results of some mappings proved useful, it was also found that the relatively few degrees of freedom present in the joysticks made it difficult for human operators to envision how joystick movements corresponded to the continuum robot motions, which often remained non-intuitive to the operator.

In this paper, we consider and demonstrate the teleoperation of continuum robots using rigid-link manipulators as input devices. The key innovation is to exploit the higher degrees of freedom (relative to conventional joysticks) of the rigid link manipulators, to more intuitively map their movements to those of continuum robots. We synthesize and implement a series of novel mappings between the input and output devices, and evaluate their effectiveness via tests in the laboratory using a test participant group. The results indicate that rigid-link manipulators can be an effective means to intuitively teleoperate continuum robots. They also suggest that operator performance is not strongly linked to either previous robotics or gaming experience.

The paper is organized as follows. The following section describes the hardware system used in the research. Section III introduces and discusses the series of mappings developed and demonstrated using the system, focusing on their intended goal of making teleoperation more intuitive. The design and implementation procedure for evaluation studies using the mappings is described in section IV, with corresponding experimental results presented in section V. Discussion and conclusions are contained in sections VI and VII, respectively.

II. The System

Driven by the inherent difficulty in understanding the operation of continuum robots, we sought to use a non-traditional approach to continuum robot control, using a non-redundant, rigid-link robotic arm as a teleoperative input device. The design of this experiment merges the two distinct topologies of rigid-link and continuum robotics with the

intent of creating an intuitive relation that allows users to control continuum robots using rigid-link systems. This scheme gives the user physical control of a widely available system type with anthropomorphic kinematics in order to manipulate a more specialized device with more complex and less intuitive kinematics.
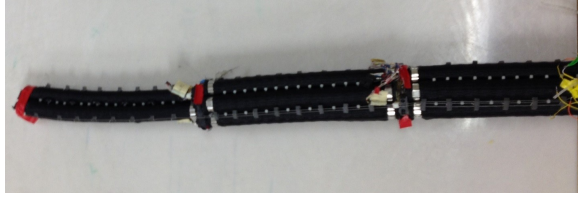

Fig. 1. The 9 Degree-of-Freedom OctArm Manipulator

A. Continuum Robot Manipulator

In this study, the continuum system used was the OctArm [35], a redundant continuum manipulator comprised of three distinct sections. The sections are designated as the base, middle, and tip, pictured right to left in Figure 1. Each section was capable of three independent motions: change in section length, change in section curvature, and change in orientation in three dimensional space. These variables are designated by $s(t)$, $\kappa(t)$, and $\phi(t)$, respectively. The total system has 9 (DoF).
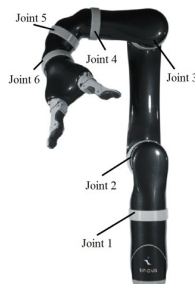

Fig. 2. The 6 Degree-of-Freedom Kinova Mico Research Arm

B. Rigid Link Robot Controller

As our chosen teleoperative controller, we used a Kinova Mico Research Arm [36]: a non-redundant, rigid link arm with 6 DoF, shown in Figure 2. The Mico Arm was chosen because it is representative of the large range of anthropomorphic robotic arms and its size allows for easy manipulation by a human user. During experiments, the Mico Arm was placed in "float" mode, which allowed the user to manipulate the arm freely while the robot automatically compensated for gravity at each joint. Joints 2 and 3 have physically limited rotation (Joint 2 rotates between 35 and 325 degrees, Joint 3 is limited to rotation between 50 and 310 degrees as designated by the Mico Arm joint limit). The Mico Arm also features a gripper, but this element was not required in this study. The output of the Mico Arm in this study was a temporal series of joint angles produced by the 6 revolute joints to be mapped to the OctArm.
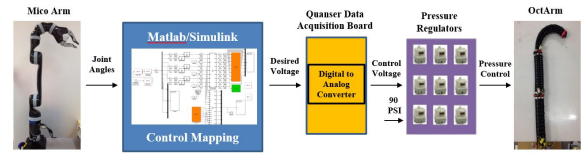

Fig. 3. Teleoperative Control Block Diagram

C. Teleoperative Control

Several schemes were devised and tested in an attempt to learn the most intuitive control for the OctArm. Figure 3 depicts the control layout from the user through the Mico Arm and mapping software, and finally to the OctArm. As seen, each test in the experiment can be broken into the following four steps:

First, the user physically manipulated the Mico Arm by rotating any of the six available joints. Several joints could be manipulated at once or each joint could be operated independently.

While the user manipulated the Mico Arm, the Kinova control software continually read each joint angle serially via a wired USB connection. The joint values then passed internally via a network socket to a Simulink model that controlled the OctArm.

The third step occured within the Simulink model. The model designated how each of the Mico Arm joints was mapped to the movement of the OctArm. Using the 6 joint angles from the Mico, the model passed the values through function blocks that converted the joint angles into a combination of $s(t)$, $\kappa(t)$, and $\phi(t)$ values for each section of the OctArm. These mappings, and their effectiveness in providing intuitive teleoperation of the OctArm, are the focus of this paper and are detailed further in Section III.

Once the nine OctArm DoFs were calculated, they passed through another function block that calculates the necessary lengths for each actuator muscle within the different sections of the OctArm and the necessary pneumatic pressure to acquire each length. The individual pneumatic pressures were passed to the corresponding pressure regulators as an analog control voltage through the use of a Quanser data acquisition board [37]. These pressures caused the OctArm to assume the configuration designated by the Mico Arm joint angles.

III. Control Mapping

As the focus of this study was intuitive control of redundant continuum systems, it was important to develop control mappings between the OctArm and Mico Arm that would be easily understood by users. For both the planar and spatial motion experiments described in this paper it was important to maintain a consistent organization between the configuration of the OctArm and that of the Mico Arm when designing each mapping. This reason was why for all future references in this paper, the base of the OctArm was assigned to correspond to the base of the Mico Arm, or Joint 1, and the tip of the OctArm was related to the end effector of the Mico Arm, or Joint 6.

A. Planar Motion Mappings

The first series of experiments conducted in this study limited the OctArm to a single plane of motion. This limitation restricted the OctArm to 6 DoF ($s(t)$ and $\kappa(t)$ for each of the three sections). In addition to the 6 DoF, two values of $\phi(t)$ were available for each section. These values dictated whether the section curved left or right in the plane with respect to the end of the previous section. The values of $\phi(t)$ did not impact the user or influence the layout of the mappings. Thus the ratio of DoF became a 1-to-1 ratio between the Mico Arm and the OctArm. The planar mappings were developed to assign a single OctArm value, $s(t)$ or $\kappa(t)$, to each joint of the OctArm while keeping the previously established orientation. The available values of $\phi(t)$ were controlled by the same joint of the Mico Arm as the $\kappa(t)$ value of the same OctArm section. There were 4 mappings developed for the planar experiments, as described in Table I.

1) Planar Mapping 1 (P1): Mapping P1 of the planar experiments explored the idea of having the Mico Arm divided into operational sections similar to the OctArm. In this particular scheme, Joint 1 and Joint 2 together control the Base section, Joint 3 and 4 control the Middle section, and finally Joint 5 and 6 control the Tip section. For all pairings, $\kappa(t)$ was controlled by the first joint and $s(t)$ was controlled by the second joint. The idea behind this scheme derived from the similarity in section assignment of the controller to the inherent section division of the OctArm manipulator.

2) Planar Mapping 2 (P2): In mapping P2, instead of dividing the Mico Arm into sections according to OctArm section assignment, the joints were grouped by the OctArm variables available, $s(t)$ and $\kappa(t)$. Joints 1, 2, and 3 of the Mico Arm controlled the $\kappa(t)$ value for the Base, Middle, and Tip section, respectively. Similarly, Joints 4, 5, and 6 controlled $s(t)$ for each OctArm section in order from Base to Tip section. It was predicted that P2 would receive the highest intuition rating due to the physical constraints of the Mico Arm. The limitations of Joints 2 and 3 gave the two joints natural midpoints (180 degrees) for the value of $\phi(t)$ to alternate between its two planar values per section. The midpoint for both joints was easily discernible because it resulted in a straight line connecting the segments on both sides of each joints. Thus, the physical design of the Mico Arm was thought to increase the intuition of this mapping.

3) Planar Mapping 3 (P3): Mapping P3 was an adaptation of Mapping 2. In this mapping, the $s(t)$ values were assigned to Joints 1, 2, and 3. $\kappa(t)$ was controlled by Joints 4, 5, and 6. This mapping was expected to enable performance with some ease but not as intuitively as P2. The idea of having all $s(t)$ values and all $\kappa(t)$ values grouped together allows manipulation of shape using a small group of Mico joints, as opposed to the use of almost the entire Mico Arm as in P1.

4) Planar Mapping 4 (P4): The final mapping, mapping P4, is an adaptation of P1. In this mapping, the order of $s(t)$ and $\kappa(t)$ per section assignment were reversed; $s(t)$ is the first joint in each grouping of two Mico joints and $\kappa(t)$

Mico Joint	P1	P2	P3	P4
1	$\kappa(t)_{Base}$	$\kappa(t)_{Base}$	$s(t)_{Base}$	$s(t)_{Base}$
2	$s(t)_{Base}$	$\kappa(t)_{Mid}$	$s(t)_{Mid}$	$\kappa(t)_{Base}$
3	$\kappa(t)_{Mid}$	$\kappa(t)_{Tip}$	$s(t)_{Tip}$	$s(t)_{Mid}$
4	$s(t)_{Mid}$	$s(t)_{Base}$	$\kappa(t)_{Base}$	$\kappa(t)_{Mid}$
5	$\kappa(t)_{Tip}$	$s(t)_{Mid}$	$\kappa(t)_{Mid}$	$s(t)_{Tip}$
6	$s(t)_{Tip}$	$s(t)_{Tip}$	$\kappa(t)_{Tip}$	$\kappa(t)_{Tip}$

TABLE I

VARIABLE MAPPINGS FOR PLANAR MOTION

Mico Joint	S1	S2	S3
1	$s(t)_{Base}$, $\kappa(t)_{Base}$	$s(t)_{Base}$, $\kappa(t)_{Base}$	$\phi(t)_{Base}$
2	$\phi(t)_{Base}$	$s(t)_{Mid}$, $\kappa(t)_{Mid}$	$s(t)_{Base}$, $\kappa(t)_{Base}$
3	$s(t)_{Mid}$, $\kappa(t)_{Mid}$	$s(t)_{Tip}$, $\kappa(t)_{Tip}$	$s(t)_{Mid}$, $\kappa(t)_{Mid}$
4	$\phi(t)_{Mid}$	$\phi(t)_{Base}$	$\phi(t)_{Mid}$
5	$s(t)_{Tip}$, $\kappa(t)_{Tip}$	$\phi(t)_{Mid}$	$\phi(t)_{Tip}$
6	$\phi(t)_{Tip}$	$\phi(t)_{Tip}$	$s(t)_{Tip}$, $\kappa(t)_{Tip}$

TABLE II

VARIABLE MAPPINGS FOR SPATIAL MOTION

is second. This mapping was expected to perform similarly to P1 in intuitiveness using the appeal of Mico sections to control OctArm sections.

B. Spatial Motion Mappings

The Spatial Motion experiments give the OctArm the full range of motion, creating a 6-to-9 DoF ratio between the Mico Arm and the OctArm. This presented a unique problem of obtaining multiple distinct signals from the joints of the Mico Arm in a consistent way that allows for intuitive control of the OctArm. In developing the spatial motion mappings, the values of $s(t)$ and $\kappa(t)$ were chosen to share a single joint as opposed to the $\kappa(t)$ and $\phi(t)$ relationship used in the planar experiments. $\phi(t)$ for each OctArm section was given its own Mico Arm joint because the range of $\phi(t)$ is 0 to 360 degrees of revolution, which gives a 1-to-1 relation to the revolute joint angles. Using the fact that the Mico Arm outputs joint angles, a solution was devised through the use of sinusoids of two different frequencies in order to transform the joint angle into a range from 0 to 2 that was then scaled to the maximum and minimum $s(t)$ and $\kappa(t)$ values for each prescribed OctArm section. The values of $s(t)$ and $\kappa(t)$ were calculated using the following equations:

$$s(t) = s(t)_{min} + (s(t)_{max} - s(t)_{min})\frac{\sin(4\theta_i) + 1}{2} \quad (1)$$

$$\kappa(t) = \kappa(t)_{min} + (\kappa(t)_{max} - \kappa(t)_{min})\frac{\sin(\theta_i) + 1}{2} \quad (2)$$

where θ_i is the angle output of Joint i and $s(t)_{min}$, $s(t)_{max}$, $\kappa(t)_{min}$, and $\kappa(t)_{max}$ are the minimum and maximum

values of $s(t)$ and $\kappa(t)$, respectively. Three mappings were developed using these techniques and equations. Table II summarizes the breakdown of each spatial mapping.

1) Spatial Mapping 1 (S1): The first spatial motion mapping was an extension of Mappings P1 and P4 of the planar motion experiments. Joints 1 and 2 of the Mico Arm controlled the three values of the Base section of the OctArm, Joints 3 and 4 controlled the Middle section, and Joints 5 and 6 controlled the Tip section. Within the groupings, $s(t)$ and $\kappa(t)$ were assigned to the first joint and $\phi(t)$ to the second. This mapping was predicted to be the least intuitive of the proposed solutions. The main reason for this prediction was the fact that $\phi(t)$ for the Base section was assigned to Joint 2 of the Mico Arm. This meant that a variable signifying the 360 degree rotation of the OctArm section in space was controlled by a joint that could only rotate 260 degrees. Thus, the Base section would not be able to continuously rotate to any direction.

2) Spatial Mapping 2 (S2): Similar to S1, mapping S2 was derived from the planar experiment mappings; in this instance mappings P2 and P3. The $s(t)$ and $\kappa(t)$ values were controlled by Joints 1, 2, and 3 and $\phi(t)$ was controlled by Joints 4, 5, and 6. Similar to the planar versions, S2 was predicted to perform with greater intuitiveness than S1. In the spatial motion of the OctArm, the two most important factors are the orientation and shape. Isolating $s(t)$ from $\kappa(t)$ was not critical due to the redundancy and availability of multiple solutions. S2 therefore isolates the two major factors into distinct groups, allowing the user to easily locate which group of factors they need, shape or orientation.

3) Spatial Mapping 3 (S3): Mapping S3 was an alteration of S1 that was intended to correct for the discontinuity of $\phi(t)$ for the Base section. The Base section was still controlled by Joints 1 and 2, the Middle section by Joints 3 and 4, and the Tip section by Joints 5 and 6. The joint pairs controlling the Base section and Tip section had $\phi(t)$ controlled by the first joint and $s(t)$ and $\kappa(t)$ values controlled by the second joint. The Middle section differed by having $\phi(t)$ controlled by the second joint (Joint 4) and $s(t)$ and $\kappa(t)$ controlled by the first joint. This mapping ensured that $\phi(t)$ was assigned to a revolute joint without physcial limits. The anticipation of this mapping was that it would be more intuitive than S1 but still less intuitive than S2 because of the switch in OctArm variable control order.

IV. STUDY DESIGN

A study was designed to step participants through a series of tasks that evolve in complexity in order to develop a procedure for systematically evaluating the control of the OctArm. This procedure was created to test the full range of each mapping in section III and to force the participants to use every joint of the Mico Arm to reach the solutions. The study comprised of two separate parts, planar and spatial motion manipulation. The overall study used a group of 15 participants to test the mappings, 7 tested planar teleoperation and 8 tested spatial teleoperation. Participants volunteered from among students and faculty of Clemson University with a wide range of academic backgrounds and areas of study. Demographic details of the participants are given in section V-A.

A. Planar Motion Study Goals

The main focus of the planar experiments was the establishment of the baseline feasibility of using a rigid-link robotic arm as a viable, intuitive control device for a continuum robot. The use of outside participants was expected to give us insight into the following questions:

1. Can a rigid-link robot with a 1-to-1 DoF relation be reliably used to control a continuum robot in planar motion?

2. Is there an intuitive control mapping solution set that can be used by the general public? If so, which of the developed mappings most fulfills this goal?

3. Is there an advantage to using such a teleoperative solution in controlling continuum robots over using a kinematically-similar controller?

B. Spatial Motion Study Goals

The Spatial Motion portion of this study took place after the conclusion of the planar experiments, which led to a development of new study questions and goals. The main goal of the spatial motion trials comprised of an attempt to find the most intuitive and universal solution to the teleoperation of general 3D motions of continuum robots using the rigid-link system. The following research questions were developed for the spatial motion trials:

1. Can a non-redundant system adequately be used to control a kinematically redundant continuum system?

2. Does robotic or gaming experience have an impact on intuitive use of such control mappings?

3. Is there a spatial motion mapping solution developed in this study that could be applicable to the general public?

C. Study Setup

In the establishment of this study, it was important to create a consistent plan for the execution of experiments to be used for both the planar and spatial motion experiments. We ensured that the subjects received the same set of instructions in order to perform the assigned tasks, whether they were planar or in 3D space. Thus, each participant underwent the same three phases for each of the available mappings:

1. Warm Up Phase
2. Task Phase
3. Evaluation Phase

In conjunction with the physical testing, participants were asked to complete a non-invasive and anonymous questionnaire that asked about video gaming experience, robotic experience, and field of academic study. For this, we obtained study approval from the Institutional Review Board (IRB) concerning the acquistion of participant information. At no point in the study were the mappings of the Mico Arm joints to the OctArm values disclosed to the participants in the

study, the goal being to preserve the evaluation of intuitive control. Each volunteer in the study tested every mapping for either planar or spatial motion and the order in which mappings were tested was kept consistent for all participants. The order of testing was determined by the order in which the mappings were created.

Prior to the beginning of the experiment, each participant was given a brief introduction to the OctArm and Mico Arm which detailed what movements the participants could expect to see and what configurations both the Mico Arm and OctArm were capable of reaching. Next, the participants were instructed to manipulate the Mico Arm without the OctArm running in order to gauge the amount of force necessary to rotate each joint of the arm and understand the complete range of motion capable of the Mico Arm joints.

1) Warm Up Phase: The Warm Up Phase of the experiment was the first introduction of the participant to actually controlling the OctArm. For each mapping used, either four for Planar or three for Spatial Motion, in the experiment, the participant was given approximately 5 minutes, or less if they declared readiness, to experiment with each joint of the Mico Arm and observe the corresponding reaction of the OctArm. During the warm up phase participants were allowed to write down observations or guesses at the layout of each mapping in order to help remember the order of Mico Arm joint assignments during the following phases of the experiment.

2) Task Phase: During the Task Phase the participant was given a series of OctArm shapes to create or goals to achievel using the OctArm. In the Planar experiments, the participants were tasked to form four shapes, seen in Figure 4, each evolving a higher complexity manipulation of both the OctArm and Mico Arm than the previous shape. The final task of the Planar experiment was to move the end of the Tip section to an X marked on the plane on which the OctArm rested during that portion of the study.

In the Spatial Motion study, participants were given only three tasks for each mapping, depicted in Figure 5. The first task tested the user for control of $\phi(t)$ by having the participant orient each section of the OctArm so that they all curved into the same plane. The second task tested control of all 9 OctArm DoF by having the end-effector of the OctArm once again reach an X marked on a board placed close to the OctArm. This second task had several possible solutions, but the awareness of $s(t)$ and $\kappa(t)$ were important in having the end effector at the correct height. The final task tested for an in-depth understanding of all 9 DoF. For this task, a marker was fixed to the end of the Tip Section of the OctArm. The participant was then tasked with drawing a straight, vertical line on the white board that contained the X from task 2.

During the Task Phase, participants were offered coaching to complete tasks, for example advice about increasing the curvature of a particular OctArm section, without stating which joint of the Mico Arm they needed to manipulate to follow the council. Participants were video recorded performing the tasks to help analyze the approaches users took to problem solving with the OctArm. Additionally,

1st Task: Return to Straight Line

2nd Task: Curve Tip Section

3rd Task: All Sections Curve in Single Direction

4th Task: Alternate Directions of Curve

Fig. 4.   Orientation Based Tasks for Planar Motion Study

1st Task: Planar Orientation of Sections

2nd Task: Place End of OctArm to Target X

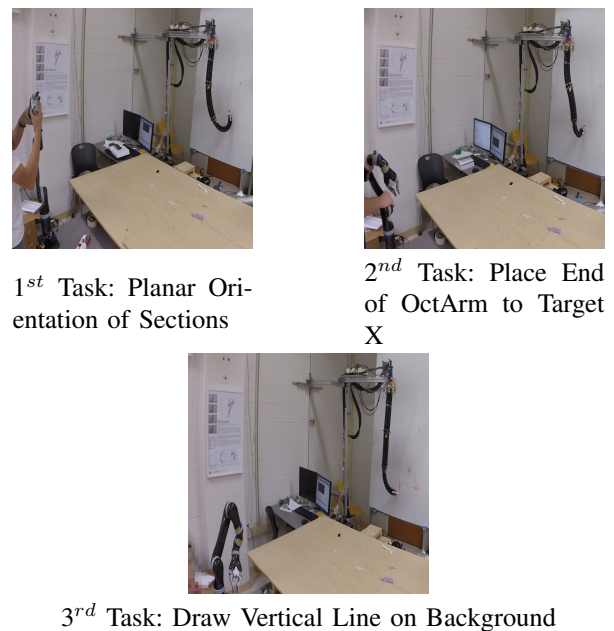3rd Task: Draw Vertical Line on Background

Fig. 5.   Task Phase of Spatial Motion Study

during the Task Phase, participants were given a time limit to perform each task, motivated by the idea that intuitive control should be quick to learn. This limit was 5 minutes for the planar motion tasks and 10 minutes for the spatial motion tasks. The Spatial Motion limit was set longer due to the redundancy of the OctArm and the presence of several solutions to each task.

3) Evaluation Phase: In the Evaluation Phase the participants completed a final questionnaire at the conclusion of the experiment. For each mapping in the experiment, there were two questions. The first question requested participants give

each mapping a rating, with choices: intuitive, usable, usable with practice, difficult to use, and unusable. The participants were then asked to evaluate how they believed the general public would perform while using each of the mappings, using the same scale from the first question.

V. EXPERIMENTAL RESULTS

The main evaluation criteria from this study fall into three categories. First, we used the results from the questionnaire for both the planar and spatial motion experiments. This mode presents the most detailed evaluation of how participants viewed the control mappings. Secondly we analyzed the data regarding the completion of tasks within the time constraints; for a control scheme to be truly intuitive the user must be able to complete assigned tasks in a timely manner. The third catergory we used for evaluation was the analysis of the correlation between user performance and video gaming or robotics background.

A. Questionnaire Results

This section presents all of the information collected in both the initial questionnaire and the evaluation of the mappings from each participant. The results are present for both the planar and spatial motion experiments.

The total number of participants for the study was 15; 7 were used in the planar motion study and 8 participated in the spatial motion experiments. There were 4 participants that took part in both the planar and spatial motion experiments. Of the 15 participants, 8 were male, 7 were female.

In the planar motion study, all 7 participants reported having little or no previous experience with robotics, only 2 were noted to have any experience at all. However, all participants but one in the planar study claimed to have video gaming experience, though at varying lengths of experience from one year up to 15 years. Four of the eight free spatial motion participants reported having robotic experience and all reported having some level of video game experience. The ages of the participants ranged from 18 to 30 years of age, with the majority being between 18 and 21.

The results of the planar mapping evaluations are shown in Figure 6. The evaluations were scaled to range from 0 to 4, where 0 indicates an unusable control mapping and 4 indicates an intuitive control mapping between the Mico Arm and OctArm. Displayed in the table are the average ratings the participants gave based on their performance and how well they thought the general population would do with the control mappings. Additionally displayed is the standard deviation for each mapping. Figure 7 displays the corresponding information for the Spatial Motion experiments.

In the planar experiments, mapping P2 received the highest rating for both Self Evaluation ($M = 3$, $SD = 0.92$) and General Population ($M = 2.43$, $SD = 0.73$). P3 and P4 in the planar experiments earned the same average Self Evaluation rating ($M = 2.71$) but P3 had a smaller deviation ($SD = 0.83$) than P4.

The results of the spatial motion questionnaires revealed mapping S2 to have the highest average for the Self Evalu-
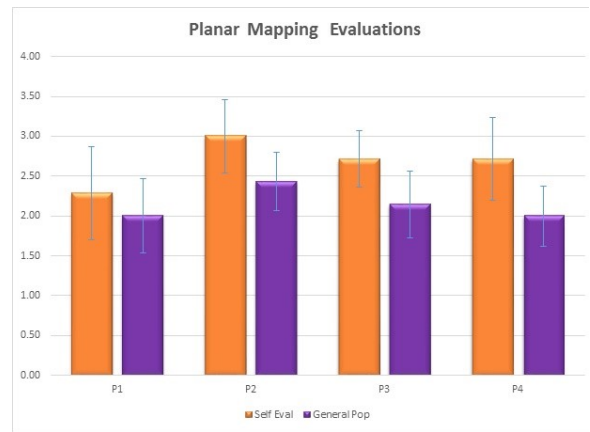

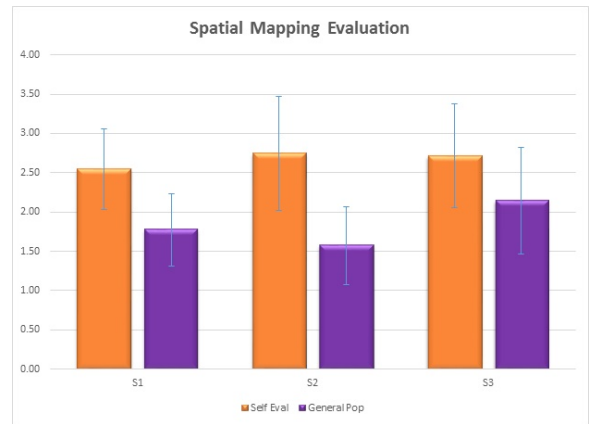Fig. 6.   Average and Standard Deviation of Planar Mapping Evaluations

Fig. 7.   Average and Standard Deviation of Spatial Mapping Evaluations

ation ($M = 2.74$, $SD = 1.46$) but S3 was rated to be better for the general population ($M = 2.14$, $SD = 1.36$).

B. Task Completion

In the planar experiments, nearly all participants were able to complete the 5 tasks for each of the 4 mappings. This part of the study had a 85.7% completion within the designated time limit. There was one participant that failed to complete each task for all 4 mappings in the allotted time. In the spatial motion experiments, some participants failed to complete all of the assigned tasks within the allotted time. Table III displays the completion percentage for each mapping and for each of the assigned tasks.

It can be seen that mapping S2, while receiving the highest Self Evaluation rating, had the lowest completion percentage of the 3 mappings. Mappings S1 and S3 were the most

Task	S1	S2	S3
1	88	75	88
2	75	75	75
3	75	63	75

TABLE III

COMPLETION PERCENTAGE FOR EACH SPATIAL MAPPING

successful of the mappings, with equal completion for all 3 tasks.

VI. DISCUSSION

The operation of the system worked well emough for us to preliminarily evaluate our goals. The majority of participants were able to complete the desired tasks, both in planar and spatial motion, well within the desired time. The teleoperative system did experience lag between the manipulation of the Mico Arm and the motion of the OctArm, this lag is an expected challenge when working with teleoperative control. In this study, the lag was the result of signal filtering of the Mico output in order to reduce noise produced by the serial passing of joint angles and did not affect the users ability or completion time.

A. Expected Results

In the overall study, our goal was to create an intuitive control mapping that allowed novice robot users to control a continuum robotic system with ease. In viewing the results from the planar experiments we achieved success in creating control mappings that nearly all participants could use to reliably control the OctArm. As predicted, mapping P2 had the most success in providing participants with intuitive control. However, the ratings P2 received were only marginally above those of both P3 and P4. In general, the fact that the remaining mappings were also rated as reasonably useable encourages the idea that, for the planar application of this system, rigid-link teleoperation of a continuum system is a viable solution, though not necessarily perfectly intuitive.

In the spatial motion experiments, the results of the study were less clear. Though some participants were highly successful in completing tasks and using the system, the evaluations received from participants were contradictory. Mapping S2 received the highest rating for self-evaluation but S3 was rated to be the easiest for use by the general public. S1 was the lowest in both categories, which fit with our prediction. The combination of $s(t)$ and $\kappa(t)$ together created some challenges for participants because of the sensitivity of OctArm responses to the $s(t)$ value. In equation (1), which calculated $s(t)$ for each section, the choice to have $s(t)$ complete four cycles for one cycle of $\kappa(t)$ was meant to create several combinations of the two values, providing more possible configurations to the user. In the actual implementation, this coupling caused the sections of the OctArm to change length too quickly for some participants to find a precise solution in a short amount of time. A solution to this would be to reduce the frequency of the $s(t)$ cycle and test which ratio of $s(t)$ to $\kappa(t)$ cycle provides the best response.

B. Experience Impact

During the experiments and after analyzing the participant demographic, it was suggested that prior robotic experience or prior gaming experience had little to no impact on participants intuitive ability to use the system. However, due to the small number of participants and the inability to create two distinct groups of experienced and inexperienced volunteers, further testing would be required to make definitive claims with respect to this question.

VII. CONCLUSION

This paper investigates the novel solution to the teleoperation of continuum robots through the use of a rigid-link robot as the control device. The study investigated the use of such a system in both planar and spatial motion. Fifteen volunteers tested the developed control mappings in order to gauge the intuitiveness of such a system. The teleoperation control scheme proved to be successful in allowing novice robotic users effective control of a continuum robot. There was no obvious relation between the robotic or video gaming experience of the participants and their success in manipulating the continuum robot. Though no mapping was universally intuitive, the results suggest that the use of rigid-link robots as teleoperative controllers is viable for continuum systems. Future work will explore the refinement of the mappings from this study and the comparison of such control schemes to that of more kinematically compatible controllers. Accompanying this paper is a video of the warm up and task phase of the planar and spatial study, including comparisons of participant completion times based on their demographic background.

REFERENCES

[1] G. Niemeyer, C. Preusche, and G. Hirzinger, *Telerobotics*. Germany: Springer, 2008.
[2] G. Robinson and J. Davies, "Continuum robots - a state of the art," in *Proc. IEEE Int. Conf. Robot. Autom.*, Detroit, MI, 1999, pp. 2849–2854.
[3] D. Trivedi, C. Rahn, W. Kier, and I. Walker, "Soft robotics: Biological inspiration, state of the art, and future research," *Applied Bionics and Biomechanics*, vol. 5, no. 2, pp. 99–117, Jun. 2008.
[4] R. Webster III and B. A. Jones, "Design and modeling of constant curvature continuum robots," *Int. Jour. Robots. Res.*, vol. 29, no. 13, pp. 1661–1683, Jul. 2010.
[5] I. Walker, "Continuous backbone "continuum" robot manipulators: A review," *ISRN Robotics*, vol. 2013, no. 1, pp. 1–19, Jul. 2013.
[6] E. Butler, R. Hammond-Oakley, S. Chawarski, A. Gosline, P. Codd, T. Anor, J. Madsen, P. Dupont, and J. Lock, "Robotic neuro-endoscope with concentric tube augmentation," in *Proc. IEEE/RSJ Int. Conf. Intel. Robot. Syst.*, Vilamoura, Portugal, 2012, pp. 2941–2946.
[7] Y. Chen, J. Liang, and I. Hunter, "Modular continuum robotic endoscope design and path planning," in *Proc. IEEE Int. Conf. Robot. Autom.*, Hong Kong, China, 2014, pp. 5393–5398.
[8] N. Simaan, R. Taylor, and P. Flint, "A dextrous system for laryngeal surgery," in *Proc. IEEE Int. Conf. Robot. Autom.*, New Orleans, LA, 2004, pp. 351–357.
[9] R. Buckingham, "Snake arm robots," *Ind. Robot: An Int. Jour.*, vol. 29, no. 3, pp. 242–245, Mar. 2002.
[10] J. Mehling, M. Diftler, M. Chu, and M. Valvo, "A minimally invasive tendril robot for in-space inspection," in *Proc Biorobotics Conference*, Pisa, Italy, 2006, pp. 690–695.
[11] M. Tonapi, I. Godage, A. Vijaykumar, and I. Walker, "Spatial kinematic modeling of a long and thin continuum robotic cable," in *Proc. IEEE Int. Conf. Robot. Autom.*, Seattle, WA, 2015, pp. 3755–3761.
[12] C. Laschi, B. Mazzolai, V. Mattoli, M. Cianchetti, and P. Dario, "Design of a biomimetic robotic octopus arm," *Bioinsp. and Biomim.*, vol. 4, no. 1, pp. 1–8, Jan. 2009.
[13] D. Lane, B. Davies, G. Robinson, D. O'Brien, J. Sneddon, E. Seaton, and A. Elfstrom, "Aspects of the design and development of a subsea dextrous grasping system," *IEEE Jour. Ocean. Eng.*, vol. 24, no. 1, pp. 96–111, Jan. 1999.
[14] B. Jones and I. Walker, "Kinematics of multisection continuum robots," *IEEE Trans. Robot.*, vol. 22, no. 1, pp. 43–57, Feb. 2006.

[15] T. Mahl, A. Hildebrandt, and O. Sawodny, "A variable curvature continuum kinematics for kinematic control of the bionic handling assistant," *IEEE Transactions on Robotics*, vol. 30, no. 4, pp. 935–949, 2014.

[16] G. Chirikjian, "Hyper-redundant manipulator dynamics: A continuum approximation," *Adv. Robot.*, vol. 9, no. 3, pp. 217–243, Jun. 1995.

[17] R. Kang, A. Kazakidi, E. Guglielmino, D. Branson, D. Tsakiris, J. Ekaterinaris, and D. Caldwell, "Dynamic modeling of a hyper-redundant octopus-like manipulator for underwater applications," in *Proc. IEEE/RSJ Int. Conf. Intel. Robot. Syst.*, San Francisco, CA, 2011, pp. 4054–4059.

[18] G. Gallot, O. Ibrahimand, and W. Khalil, "Dynamic modeling and simulation of a 3-d eel-like robot," in *Proc. IEEE Int. Conf. Robot. Autom.*, Rome, Italy, 2007, pp. 1486–1491.

[19] A. Marchese, R. Tedrake, and D. Rus, "Dynamics and trajectory optimization for a soft spatial fluidic elastomer manipulator," in *Proc. IEEE Int. Conf. Robot. Autom.*, Seattle, WA, 2015, pp. 2528–2535.

[20] H. Mochiyama and T. Suzuki, "Kinematics and dynamics of a cable-like hyper-flexible manipulator," in *Proc. IEEE Int. Conf. Robot. Autom.*, Taipei, Taiwan, 2003, pp. 3672–3677.

[21] E. Tatlicioglu, I. Walker, and D. Dawson, "Dynamic modeling for planar extensible continuum robot manipulators," *Int. Jour. Robot. Autom.*, vol. 24, no. 4, pp. 1087–1099, Apr. 2009.

[22] M. Mahvash and P. Dupont, "Stiffness control of a continuum manipulator in contact with a soft environment," in *Proc. IEEE/RSJ Int. Conf. Intel. Robot. Syst.*, Taipei, Taiwan, 2010, pp. 863–870.

[23] D. Rucker, B. Jones, and R. Webster III, "A model for concentric tubes continuum robots under applied wrenches," in *Proc. IEEE Int. Conf. Robot. Autom.*, Anchorage, AK, 2010, pp. 1047–1052.

[24] J. Li and J. Xiao, "Task-constrained continuum manipulation in cluttered space," in *Proc. IEEE Int. Conf. Robot. Autom.*, Hong Kong, China, 2014, pp. 2183–2188.

[25] L. Lyons, R. Webster III, and R. Alterovitz, "Planning active cannula configurations through tubular anatomy," in *Proc. IEEE Int. Conf. Robot. Autom.*, Anchorage, AK, 2010, pp. 2082–2087.

[26] D. Palmer and S. C.-G. D. Axinte, "Real-time method for tip following navigation of continuum snake arm robots," *Robotics and Autonomous Systems*, vol. 62, no. 10, pp. 1478–1485, 2014.

[27] L. Torres, C. Baykal, and R. Alterovitz, "Interactive-rate motion planning for concentric tube robots," in *Proc. IEEE Int. Conf. Robot. Autom.*, Hong Kong, China, 2014, pp. 1914–1919.

[28] B. Conrad and M. Zinn, "Closed loop task space control of an interleaved continuum rigid manipulator," in *Proc. IEEE Int. Conf. Robot. Autom.*, Seattle, WA, 2015, pp. 1743–1750.

[29] V. Falkenhahn, A. Hildebrandt, R. Neumann, and O. Sawodny, "Model-based feedforward position control of constant curvature continuum robots using feedback linearization," in *Proc. IEEE Int. Conf. Robot. Autom.*, Seattle, WA, 2015, pp. 762–767.

[30] R. Goldman, A. Bajo, and N. Simaan, "Compliant motion control for multisegment continuum robots with actuation force sensing," *IEEE Trans. Rob.*, vol. 30, no. 4, pp. 890–902, Apr. 2014.

[31] A. Kapadia, K. Fry, and I. Walker, "Empirical investigation of closed-loop control of extensible continuum manipulators," in *Proc. IEEE Int. Conf. Intell. Robot. Sys.*, Chicago, IL, 2014, pp. 329–335.

[32] S. Sadati, Y. Noh, S. Naghibi, and A. Althoefer, "Stiffness control of soft robotic manipulators for minimally invasive surgery (mis) using scale jamming," in *Int. Conf. Rob. and Autom.*, Amsterdam, The Netherlands, 2015, pp. 141–151.

[33] M. Yip and D. Camarillo, "Model-less feedback control of continuum manipulators in constrained environments," *IEEE Trans. Rob.*, vol. 30, no. 4, pp. 880–888, Apr. 2014.

[34] M. Csencsits, B. Jones, and W. McMahan, "User interfaces for continuum robot arms," in *Proc. IEEE Int. Conf. Intell. Robot. Sys*, Edmonton, Canada, 2005, pp. 3011–3018.

[35] M. Grissom, V. Chitrakaran, D. Dienno, M. Csencsits, M. Pritts, B. Jones, W. McMahan, D. Dawson, C. Rahn, and I. Walker, "Design and experimental testing of the octarm soft robot manipulator," in *Proc. SPIE Conf. Unmanned Sys. Tech.*, Kissimee, FL, 2006, pp. 109–114.

[36] Kinova. (2015) Kinova mico research arm. [Online]. Available: www.kinovarobotics.com/service-robotics/products/robot-arms/

[37] Quanser. (2015) Q8-usb data acquisition board. [Online]. Available: http://www.quanser.com/products/q8-usb